Chapter 2
Low-Frequency Phenomena in Swirling Flow

The presence of swirl is often the cause of separations and pressure fluctuations in the draft tube of hydraulic reaction turbines, in particular Francis turbines. At the design point, water turbines generally operate with little swirl entering the draft tube and no flow separations, but at off-design, at both high and low load, the flow leaving the turbine has a large swirling component. The present chapter describes a number of physical mechanisms that work to produce the pulsation. Their occurrence and impact depend mainly on the actual flow rate of the turbine, but also on the local pressure level, on the exit velocity field of the particular runner, the shape of the draft tube, and the dynamic response of the whole hydraulic circuit. In medium- and large-sized turbines, the frequency of these 'draft tube surges,' which are often approximately periodic, is of the order of 1 Hz, and therefore they may also produce significant electrical power swings.

Given a sufficiently strong vortex flow, comparable phenomena may also occur in other locations, for example in the runner channels, or in penstock manifolds.

2.1 Swirling Flows in Pipes, Vortex Breakdown Phenomena

2.1.1 Basic Observations

Laboratory experiments have shown that swirling flow through a cylindrical pipe tends to separate into two concentric flow regions [1]. Fluid transport basically occurs in the outer region while the inner region may contain a stagnation zone or dead water core. The relative swirl or swirl ratio is the non-dimensional ratio between the swirl momentum and the axial momentum of flow

$$m = \int_0^{R_i} c_m c_t r^2 dr \Big/ \left(R_i \int_0^{R_i} c_m^2 r dr \right) \tag{2.1}$$

P. Dörfler et al., *Flow-Induced Pulsation and Vibration in Hydroelectric Machinery*,
DOI: 10.1007/978-1-4471-4252-2_2, © Springer-Verlag London 2013

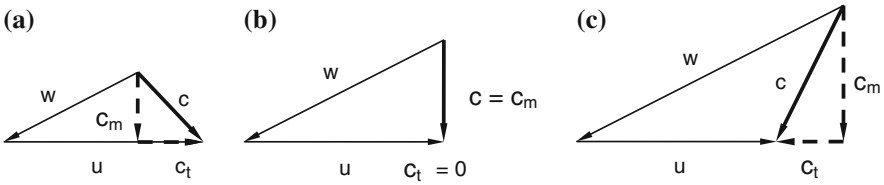

Fig. 2.1 Runner exit velocity triangles **a** partial load **b** zero swirl **c** high load

where R_i is the pipe radius, and c_m and c_t are the axial and tangential components of velocity.

Early measurements supporting the concept of two flow regions were made on a time-averaged basis [1]. The diameter of the dead water core was found to increase with the swirl rate. More detailed observations, which also consider unsteady features of flow, reveal that the boundary between the two regions, is not stable but that its vorticity tends to concentrate in a corkscrew-like vortex filament along the border between the two flow regions [2]. Under some circumstance, in particular in conditions of decelerating flow, the recirculation zone may break down from one flow structure to another, a phenomenon known as vortex breakdown or vortex bursting. The phenomenon of vortex breakdown is associated with an abrupt and drastic change of flow structure. The helical corkscrew vortex at the boundary of the core is one such structure but an alternative structure is an axisymmetric separation bubble on the axis of the vortex.

2.1.2 Early Research

In a Francis turbine, the fixed relative exit angle of the runner blades is designed for a certain water discharge. At this particular discharge, close to the point of best efficiency, the component of the absolute circumferential flow velocity in the outlet is small, leading to a residual swirl close to zero, as shown in part (b) of Fig. 2.1. At lower flows the relative flow angle remains nearly the same, but the absolute flow angle leads to a residual swirl in the direction of the runner rotation, indicated by the tangential velocity component c_t in part (a) of Fig. 2.1. At higher discharge the runner produces a counter swirl against the direction of runner rotation in its exit flow.

The US Bureau of Reclamation (USBR) conducted basic experimental research [2] on the behavior of swirling flow in a reduced-scale draft tube. Instead of a runner, a stationary swirl generating apparatus was used to produce a certain swirl ratio. At very low swirl, the USBR found that the dead water core does not develop, the smooth flow filling the entire cross section of the draft tube. If the swirl ratio exceeds a rather low threshold value, a stagnation point forms in the

Fig. 2.2 Dead water core (*left*, [3]) and corkscrew vortex in a model

flow at the draft tube exit and downstream of this there is a core of separated flow in the draft tube. This stagnation point then moves upstream as the swirl ratio increases. The stagnation point is also the starting point of the corkscrew-like vortex filament. With sufficient swirl, the stagnation point merges with the upstream center of the pipe, and the vortex filament then starts at the 'runner' hub. It is not stationary but rotates about the axis of the draft tube (Fig. 2.2).

The shape and precession frequency of the corkscrew vortex depend on the swirl ratio. This early research was done using air as a working fluid. Cavitation effects were not considered. Starting from the same concept, Nishi et al. [3] studied various aspects of swirling draft tube flow, including the effect of vortex cavitation and the role of the draft tube elbow in the excitation mechanism of pressure pulsations [4].

2.2 Draft Tube Vortex Phenomena

Today, researchers still use reduced-scale models to examine draft tube vortex phenomena, but these days complete turbine models with runner are preferred to stationary swirl generators. While the swirl apparatus can produce the proper amount of swirl, the radial distribution of velocities differs from that in an actual turbine. Several different dynamic flow phenomena due to draft tube swirl may be distinguished by their symptoms and mechanism of origin. The flow rate of the turbine controls the swirl, and has the single most important influence on the occurrence of pulsation. Therefore, it is convenient to use a non-dimensional number for the discharge to quantify this, usually $Q_{nD}/Q_{nD,opt}$. The discharge Q is a good scaling parameter only in the usual case of a turbine operating at constant, synchronous speed. But in other cases such as a model test, the discharge coefficient Q_{nD} should be used because the swirl-free discharge varies with the flow and the runner speed.

Apart from the swirl ratio and the radial velocity distribution, the cavitation number σ also plays an important role. In most cases the high velocities in the core of the draft tube vortex can decrease the static pressure to the vapor pressure, leading to cavitation with a vapor-filled cavity. Some pulsation phenomena are linked to the size and shape of the cavity. The following descriptions are given for modern Francis turbines where the condition of zero swirl normally occurs at, or slightly above, the best efficiency discharge; many of the phenomena are also observed in other reaction turbines with the corresponding draft tube swirl.

2.2.1 Partial-Load Vortex: Forced Oscillation (Half-Load Surge)

In modern Francis turbines, the corkscrew-like flow structure (vortex rope or torch) typically prevails over a range of the relative turbine discharge between approximately 0.5 and 0.85 of the flow at best efficiency. The lower limit of this range is often better developed than the upper limit as it has the character of a boundary between two quite different flow regimes. The common way to measure the effects of the phenomenon is by pressure sensors at the wall of the draft tube cone (draft tube pressure pulsation, DTPP). This pulsation is approximately periodic, the period of the pressure pulsation is the same as that for the rotation (precession) of the corkscrew, which may be observed visually in a laboratory model with a transparent draft tube cone. The relative frequency of precession f/n is between 0.2 and 0.4, whereby values above 0.3 are less likely. First results on this phenomenon, which are still worth reading, can be found in Rheingans [5] who already pointed to problems of generator resonance and proposed a generic estimate f/n $\cong$ 0.278 for the ratio of the precession frequency to the runner speed. For detailed quantitative information on surge parameters, see the Sects. 7.2.1 and 7.3.1.

In a model test, DTPP measurements can be done at different levels of draft tube pressure, or cavitation number σ as described in Sect. 1.1 (other parameters of operation remaining the same). Figure 2.3 shows results from a Francis turbine model with a specific speed of $n_{QE} = 0.113$, and these demonstrate some typical features of the cavitation effect[1] on the part-load pulsation. If the pressure level in the model draft tube is very high, $\psi\sigma \geq 0.3$, the vortex rope becomes invisible because the local pressure drop in its core is not sufficient to produce cavitation. Nevertheless the unsteadiness from the corkscrew vortex still exists in the flow and if the DTPP is measured its frequency remains approximately the same as the draft tube pressure is lowered. It is common to measure the pulsation at several locations around the circumference of the cone simultaneously. The rms values of the fundamental frequency band of the vortex precession in the draft tube cone are

[1] In the cavitation number $\psi\sigma$, different from standard σ, the reference pressure is the runner velocity head instead of the net head.

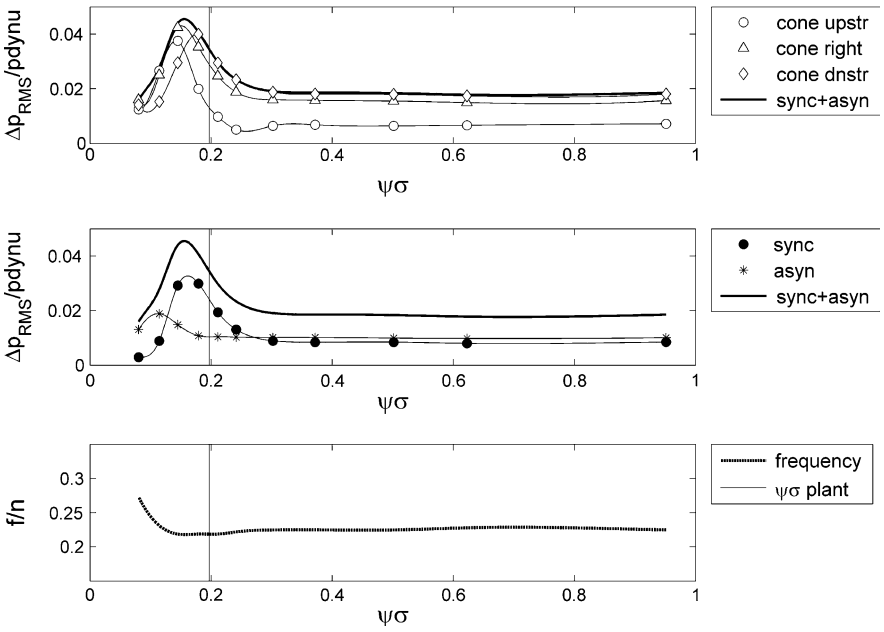

Fig. 2.3 Cavitation effect on half-load surge

shown in the upper graph of Fig. 2.3 for three locations in the draft tube cone. A maximum of the pressure amplitudes is often observed when the natural frequency of the draft tube fluid associated with the cavitation compliance of the vortex rope coincides with the precession frequency of the rope. In this condition—in our case near $\psi\sigma = 0.16$—the pressure pulsation observed at different circumferential locations becomes approximately synchronous [6]. The reason for the resonance-like behavior, already recognized by Moody [7], is the compressible nature of the flow downstream of the runner, following Brennen's [8] 'cavitation compliance' defined in Eq. (2.2). The correct mechanism of excitation was disclosed in two steps by Dériaz [9] who assumed a periodic variation of flow resistance, and Dörfler [10, 11]. The computation example in Sect. 1.4 and the system response study in Sect. 7.2.3 provide a more detailed description.

The physical properties of half-load surge—that is the amplitude and phase response to changes in cavitation level due to variation in sigma—can only be understood if the compound nature of this phenomenon is accounted for. Nishi [4] showed that the pulsation consists of a synchronous part—a plane wave—and an asynchronous part—the precession movement of the rope, and showed how these components are to be distinguished in an elbow draft tube. He also conducted experiments which demonstrated that the synchronous pulsation does not exist in a straight draft tube—another proof that the excitation source resides in the elbow. The middle graph in Fig. 2.3 presents the synchronous and asynchronous pulsation, which were extracted from the individual pressure signals. It is the

synchronous component, which is involved in a basically one-dimensional system oscillation, that responds to the change of cavitation level. In contrast the asynchronous pulsation as well as the precession frequency (lower graph) do not depend on cavitation except at extremely low draft tube pressure. The maximum possible level of pulsation in any draft tube section may be expressed as the scalar sum of the amplitudes of the two components, therefore this sum forms an envelope for the individual pressure amplitudes versus cavitation number, in the upper graph.

To analyze measurements of draft tube pulsation for its parameters, based on a set of assumptions listed in Sect. 7.2.3, one may use procedures in the frequency domain. The goal is to know in detail the properties of the two main components, asynchronous and synchronous, as well as the forcing term Δp_{EX}.[2] If the test rig has short upstream and downstream pipes as shown in Fig. 1.10, it is particularly easy to identify the pressure source Δp_{EX} by measuring the interesting load points in a reference test at partial load with high cavitation number σ in order to ensure cavitation-free flow in the runner and draft tube. This should normally be the case for $\psi\sigma > 0.5$ but can be checked during the test.

The evaluation should start with a multi-channel FFT analysis of the pressure signals upstream and downstream of the runner; if available, pulsation signals of shaft torque and discharge can also be included. The analysis should concentrate on the frequency band of vortex precession. The magnitude of all spectral lines of the frequency band should be included. The phase angles are required for the analysis; it is recommended to evaluate the coherence as a measure for signal-to-noise ratio. The synchronous pulsation p_{sync} is obtained as the (complex-valued) average of the pressure signals at equally spaced locations in one cross section of the draft tube cone. Four sensors displaced by 90° are recommended, two are minimum. The asynchronous pulsation in every pressure signal p_i results from

$$P_{asyn,\,i} = p_i - p_{sync} \tag{2.2}$$

always using the complex variables. Note that this procedure can also be used at conditions with cavitating vortex, or at high load. At partial load, it will reveal any cavitation-dependency of the asynchronous component, as shown in Fig. 2.3. At high load, there is often no coherent pulsation, or otherwise there is no significant asynchronous component.

If the system is simple, the pressure source Δp_{EX} is obtained from the measured pressure pulsation p_{SC} in the spiral casing entry and the pressure transfer function $G_{SC}(j\omega)$ between the two pressure variables. $G_{SC}(j\omega)$ differs from G_C in Eqs. (1.36) and (1.38) only in the numerator N which represents the impedance downstream of the runner, and has to be replaced by the impedance at the location of pressure sensor p_{SC}. The compliance C_C is zero in the cavitation-free reference test; therefore there are no more unknowns in the equation

[2] We are omitting the tilde; all pressure variables are fluctuations.

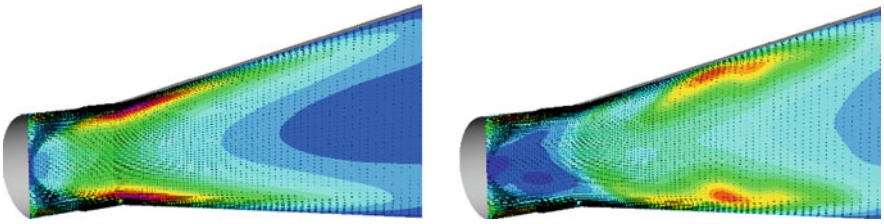

Fig. 2.4 Turbulent kinetic energy of swirling flow in a conical diffuser

$$\Delta p_{EX} = p_{SC} / G_{SC} \tag{2.3}$$

Within the accuracy of the one-dimensional system model, the same should result if the synchronous pulsation p_{sync} in the draft tube cone is evaluated first and the equations in Sect. 1.4 are directly used assuming $p_C = p_{sync}$. In theory, the torque signal could also be used but the pertinent transfer function is less accurate.

First attempts to investigate the physical nature of the draft tube vortex at part load by means of Computational Fluid Dynamics (CFD) have steadily been published since 1999. For early examples, see Ruprecht et al. [12] and Sick et al. [13]. Due to the fact that this flow is dominated by vortex structures, the turbulence model has been found to be of high importance for an accurate prediction. A comparison of CFD results obtained with the standard k-ε model and the physically better justified (but more computationally expensive) Reynolds stress model is given in Sick et al. [13] for the swirling flow in a conical diffuser. Differences between the two methods may be seen in the Fig. 2.4.

At the diffuser inlet a circumferentially uniform velocity profile is prescribed which is typical for draft tube inlet flow at part load, including radial variations of the velocity components. As a result of the swirl a strong backflow builds up in the core region of the diffuser, left-hand side of Fig. 2.4. In the shear layer between the inner backflow and the outer swirling flow, small vortices develop into the typical corkscrew-like flow instability. These flow patterns are well predicted both by a laminar flow simulation and a flow simulation with the Reynolds stress turbulence model. In case of the standard k-ε model far too much turbulent dissipation is modeled in the shear layer with the result that the vortices cannot develop. This well-known weakness of the standard k-ε turbulence model can be overcome by a modification which takes into account the stabilizing effect of stream line curvature.

Furthermore, the computational grid is of major importance for a realistic prediction of the vortex and the related pressure drop toward the vortex core, as reported by Stein [14]. A good general rule says that the vortex core should be resolved by at least 20 grid cells. If this condition is not fulfilled both the velocity gradients and the pressure drop are under-predicted.

Validation of predicted DTPP versus experimental data obtained in a model test shows that single-phase flow simulations give very good results of the frequency as well as the amplitude of the pressure pulsations. The CFD simulation reported

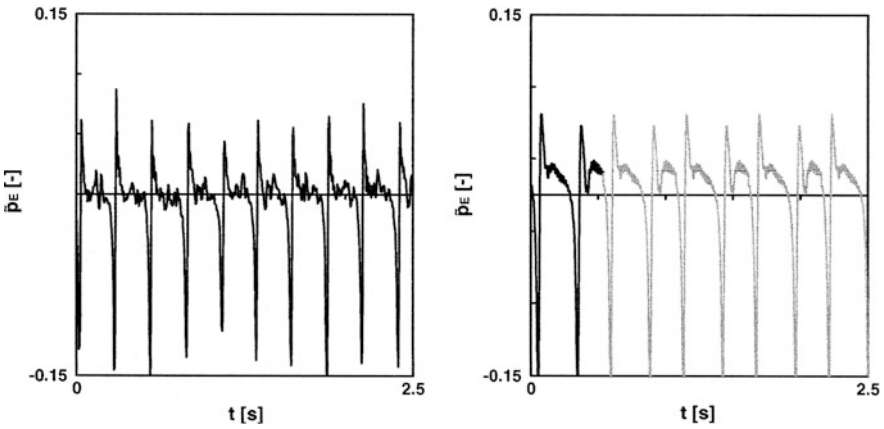

Fig. 2.5 Measured (*left*) and computed (*right*) DT wall pressure pulsation

in [14], shown in Fig. 2.5, gives a frequency prediction within 2 % accuracy compared to the measurements because very high grid resolution was used (overall 35 million nodes). For coarser computational grids, which are more common in industrial applications, the error in frequency prediction may be up to 20 %.

Two phase flow simulations reported in [14] reveal a lack of accuracy of the CFD approach with maximum 35 million grid nodes in the draft tube due to relatively low grid resolution with respect to the cavity: the volume of the cavity was under-predicted leading to a significant error of vortex dynamics prediction [14]. This suggests that numerical flow simulation can be reliably used for predicting frequency and strength of the draft tube vortex with high sigma values but not yet for predicting the effect of varying tail water level or sigma values respectively.

2.2.2 Random pulsation at Very Low Load

If the relative turbine discharge $Q_{nD}/Q_{nD,opt}$ is lower than a certain threshold, usually between 40 and 50 %, the swirl ratio is so high that the vortex rope disintegrates. A large number of unorganized smaller vortices replace the single corkscrew vortex. The DTPP loses its near-periodic behavior and has the character of a wide-band noise. The two pressure samples in Fig. 1.4 demonstrate the different flow regimes very well. While the time-domain pressure amplitude may become larger at lower load, there are often no significant narrow-band fluctuations that may result in an intense resonance.

In the operating range directly below the single-helix vortex rope, there are sometimes vortex flow structures which occur which are not as periodic as the helix but still retain, in a statistical sense, some phase relationships. This may be seen in

Fig. 7.13 in Sect. 7.2.1 where the asynchronous pulsation does not immediately disappear together with the single-helix structure (at $Q_{nD}/Q_{nD,opt} \leq 0.6$) but only gradually. The less regular vortices prevailing in this flow regime correspond to a wider range of frequencies and phase angles in the spectrum.

In addition, Fig. 7.13 shows that the relative amount of hydraulic losses of the turbine, expressed by the ratio $(Q_{ED} - P_{ED})/Q_{ED,opt}$, starts to increase significantly together with the random part of the DTPP, at the limit of the single-vortex zone. At very low load, the entire pulsation consists of random movements only.

2.2.3 Partial-Load Vortex: Two Threads (Twin Vortex)

In some Francis turbines and pump turbines there is an additional draft tube flow regime occurring adjacent to the lower boundary of the single-helix region. If this regime exists, then its range is usually quite small, approximately 5 % of $Q_{nD}/Q_{nD,opt}$. The single helix is replaced by a double helix [15], the two threads being displaced by 180 degrees. In the DTPP, this condition is easily detected due to the discontinuous increase of frequency and change of the phase relationships; the phase relationships resemble the behavior of the 2f component existing in the single-helix flow.

The presence of a central column, or shaft, in the draft tube axis occasionally promotes the formation of the double helix pattern, see [16] for an example. Another example is shown in Fig. 2.6. Pressure signals are shown for three sensors which are equally spaced around the draft tube cone of a model with $n_{QE} = 0.23$. The right-hand side shows the regular behavior with the precession of the low-pressure zone of the single vortex marked with gray arrows. At a slightly lower flow rate, the single-helix pattern is replaced by a flow regime with two vortex threads, the additional thread being indicated by the arrows drawn with broken lines. The central column in this draft tube has 0.30 times the runner exit diameter. The doubling of the vortex does not occur in the model version without a central column.

No practical problems due to the double helix phenomenon have been reported so far.

2.2.4 Low Partial-Load: Self-Excited Oscillation

Other phenomena may also lead to pulsations at partial load. A serious pulsation phenomenon occurred in a large power plant [17] with a rated head of approximately 100 m. Each one of the turbines rated 200 MW has a separate penstock. Intense pressure pulsation was observed around 30 % of the rated output, at a relative discharge $Q_{nD}/Q_{nD,opt}$ between 25 and 40 %. The upper limit approximately coincided with the lower limit of the single-helix range. The relative frequency f/n was between 0.7 and 1.0, and increased with increasing flow.

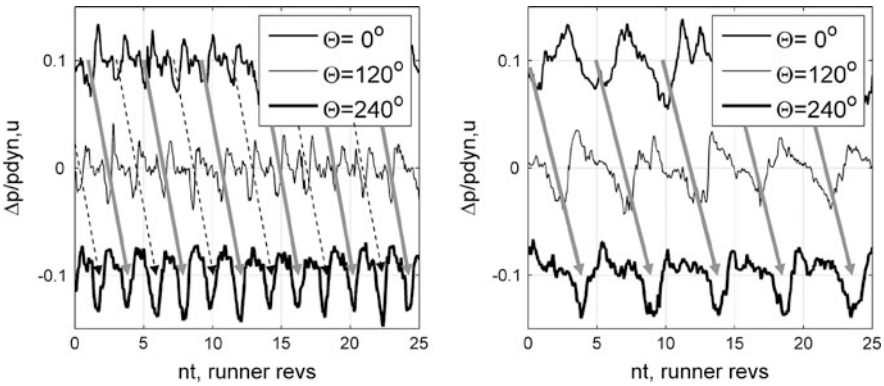

Fig. 2.6 Additional vortex thread due to central column

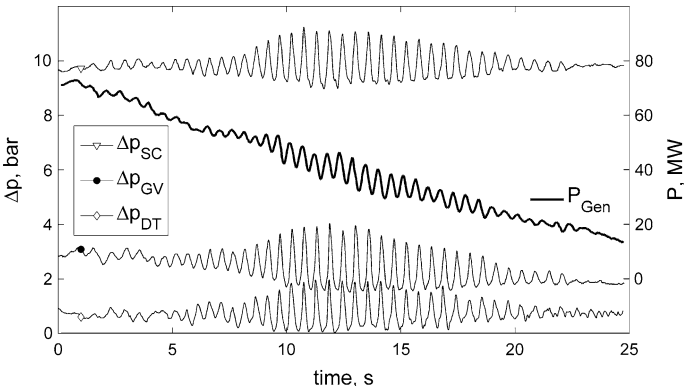

Fig. 2.7 Slow transient showing self-excited low-load pulsation

The frequency was always somewhat above the lowest natural frequency of the penstock for each one of the three units. The oscillation frequency was found to be dependent on the natural frequency determined by the penstock length (different between the units) and headwater level. The frequency range overlapped with that of the natural frequency of the generator, as a consequence there were large power swings in some situations. Figure 2.7 shows a moderate version of the phenomenon. The magnitude of pressure pulsation is roughly the same upstream and downstream of the turbine, as well as between the wicket gate and runner (Δp_{GV}). In this example, the frequency happens to coincide with the natural frequency of the generator.

No indication for the phenomenon was found in the model test, and, because of this, the oscillation is classified as self-excited. At maximum head the DTPP attained dramatic peak-to-peak values up to 63 mwc, the amplitude in the penstock being slightly smaller than in the draft tube. A variety of theories have been

proposed to explain the problem. Tentative explanations comprised a hysteresis in the turbine characteristics [18], a dead time in the vaneless space between the guide vanes and runner [18], and some system resonance responding to draft tube pressure fluctuation [17].

In a practical sense, the solution was simple. Injection of a very small air flow (85 l/s, or 0.04 % of nominal turbine discharge) through the runner hub proved to be sufficient to completely suppress the instability.

Gummer [19] described an oscillation with virtually identical properties—specific speed, load range, relative frequency, phase relationships and mode shape. In this paper, a turbine impedance with locally negative real part is supposed to be the cause. Unlike the previous example, this oscillation reportedly does not occur when the unit is ramped up. An explanation could be that the dynamic response of the two-phase flow depends on the partial pressure of the dissolved gas, which requires some time to build up.

2.2.5 *Upper Partial-Load Vortex: The "80 % Pulsation"*

In the upper partial-load range, usually between 70 and 80 % of $Q_{nD,opt}$, the half-load corkscrew vortex is often accompanied by an additional phenomenon with much higher frequency. Most observations of this phenomenon are from models with high specific speed [20–22]. The frequency spectrum typically consists of several narrow bands whose center frequencies differ by multiples of the vortex precession frequency [23]. Some examples from a Francis turbine model test are presented in Figs. 7.1, 7.2, and 7.6.

The peculiar arrangement of frequencies has been explained by a modulation process. In terms of a mathematical formula, this corresponds to multiplying two periodic functions, each one having a few harmonics:

$$X(t) = \left(A_0 + \sum_{i=1,2,..} \left(A_i \cos(i\omega_V t) + \ldots\ldots + B_i \sin(i\omega_V t) \right) \right) \times \left(C_0 + \sum_{i=1,2,...} \left(C_i \cos(i\omega_C t) + D_i \sin(i\omega_C t) \right) \right) \tag{2.4}$$

The lower frequency ω_V represents the vortex precession, while the origin of the higher frequency ω_C is not adequately explained. Arpe et al. [23] found a natural mode of the test rig to be involved; however in some tests [20] the phenomenon could be reproduced at quite different test head and speed. Other authors [24] attribute $\omega_C = 2\pi f_C$ to a precession movement of an elliptical wave shape on the vortex cavity surface. An oscillation mode with elliptical surface of the vortex has been postulated based on theoretical studies [24], and several researchers observed the revolving elliptical deformation by means of high-speed video taken in model turbines [25], and also in a model pump-turbine [26].

Relative frequencies f_C/n between 1 and 5 have been reported [20], with values close to 2.5 being most common [23]. The frequency f_C increases strongly with the draft tube pressure. Other than the pulsation at precession frequency, this component only exists when there is cavitation on the helix. The pressure pulsation may attain amplitudes in excess of the half-load vortex itself; amplitudes in the turbine intake are sometimes higher than at the draft tube cone wall.

While relative amplitudes in the model test have quite often been alarming, the phenomenon usually did not show up at the prototype turbine. Comparable phenomena in prototype units are very rare; pulsation of axial thrust felt at the thrust bearing structure has been tentatively attributed to this category in a few cases. A singular case encountered in the authors' company occurred in a turbine with a straight horizontal draft tube. In this case, the phenomenon was almost perfectly similar between model and prototype. This, and the absence of similarity in other projects, could be a hint that lack of Froude similarity (see Sects. 7.2.1 and 9.2.1) normally prevents the phenomenon from occurring in large prototypes.

In model tests, the pulsation may be suppressed by small quantities of air injected to the draft tube center. In some cases, attempts were made to minimize the 80 % pulsation in the model turbine by design modifications. These can be either changes in the contour of the runner cone (semi-tapered hub, [21]) or adjustment of the runner blade profile [22].

2.2.6 *Instability of the Helix Flow Pattern*

The corkscrew vortex is a fairly robust flow pattern occurring at partial load in virtually every Francis turbine. At the center of its range at about 2/3 of $Q_{nD,opt}$, it rotates very uniformly and regularly. However, at the limits of its range of occurrence, it may become intermittent with temporary prevalence of other (neighboring) flow patterns. During a transition between different flow regimes the vortex or parts of it may collapse. A sharp pressure shock is produced when the cavitating vortex filament suddenly implodes. Such disturbances have been observed in several model tests [27, 28], in particular near the upper limit of the range of the partial-load vortex, at 80–90 % of $Q_{nD,opt}$. The authors of [28] even called this range the 'shock zone,' when reporting about turbines with rather high specific speed.

This phenomenon has also been observed in prototype turbines where the shocks may become quite unacceptable. Different remedies have proved effective. One possibility is injection or admission of air through the runner hub. In some cases, the problem has been mitigated by adding a cylindrical extension to the runner hub, using a shape similar to the one reported as a remedy against the '80 % pulsation' [21]. For this approach, Strohmer [27], has provided a detailed description from which the content of Fig. 2.8 has been taken. In the upper graph of this figure, the draft tube pulsation in the critical range of load ($Q/Q_{opt} = 0.88$) is compared with the normal behavior at $Q/Q_{opt} = 0.62$.

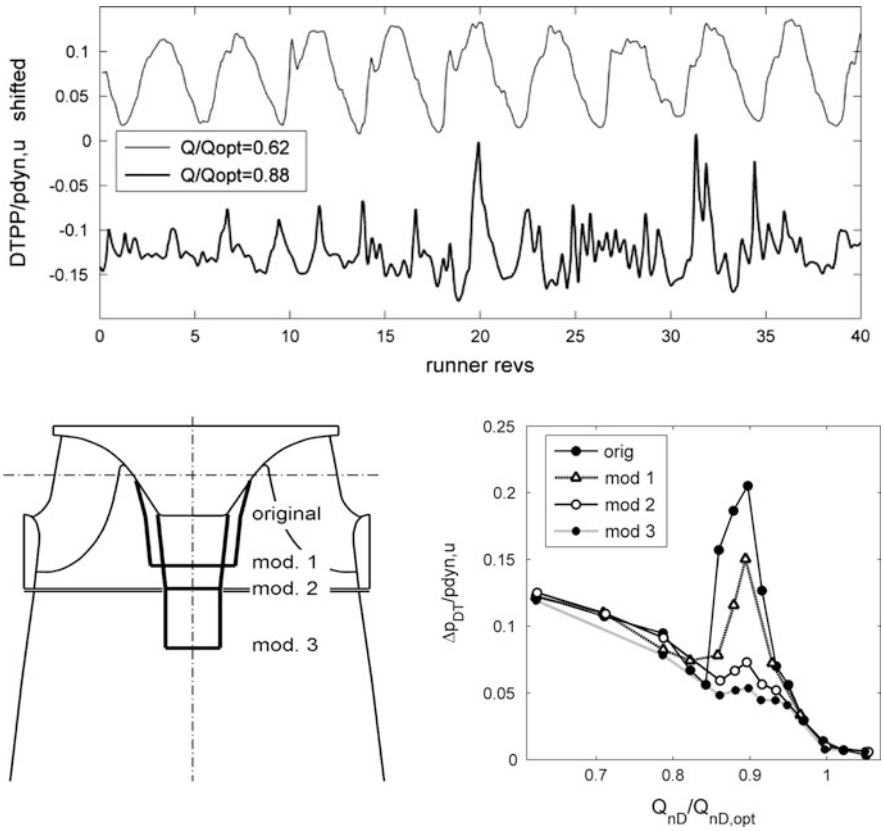

Fig. 2.8 Vortex stability enhanced by extension of hub

At $Q/Q_{opt} = 0.88$, the normal rotation of the vortex rope, with a period of about 4 runner revolutions, is no longer recognizable. Instead, there are less regular fluctuations at higher frequency and occasional pressure spikes that correspond to partial collapse of the rope. This phenomenon causes the high pressure amplitude for the original design in the lower right graph. A series of modifications of the runner hub was examined, showing that a moderate extension of the hub can rectify the problem.

2.2.7 Self-Excited Oscillation at High Load (Full-Load Surge)

In case of negative swirl at high load, the helical vortex shape occurs rather seldom. Here the vortex is usually rotationally symmetric, at least inside the upper cone region of the draft tube. Vortex precession and the accompanying asynchronous pulsation are therefore absent, as well as the forcing term of pulsation.

Nevertheless, some turbines exhibit regular and intense pulsation of pressure and power during high-load operation. This kind of surge has been explained as a self-excited oscillation. While all conventional elements used in one-dimensional fluid transient models have a damping or at least neutral effect on oscillations, the mass flow gain factor (MFGF) $\chi = -\partial V_C/\partial Q$, as explained in Sect. 1.5, has been identified as a potentially destabilizing feature connected with cavitating flows.

In the context of hydraulic turbines, the mass flow gain effect was suspected to play a role in stability for some time. Ideas to apply it to draft tube cavitation were published in the 1980s, either based on upstream flow q_1 [10], or downstream flow q_2 [29]. The latter concept has long been favored because it predicts instability in many cases. Attempts to simulate the full-load vortex were made later with steady-state CFD, in order to get more insight into the fluid dynamics and to obtain quantitative data for the mass flow gain factor (MFGF) and cavitation compliance. Flemming et al. [30] published cavity volumes estimated from single phase as well as two-phase flow simulations. The single-phase simulation estimated the cavity volume from the predicted pressure levels without cavitation (the cavity being assumed to be located in the volume where the pressure was predicted to be less than the vapor pressure), whereas the two-phase simulation calculates the cavity volume based on a certain value of the void fraction. They showed that a two-phase representation is necessary for realistic values of the cavitation parameters. The study reported, for a Francis turbine project, a gross reduction of MFGF due to replacement of single phase by two-phase parameters. It nevertheless predicted instability of the prototype turbine. Unlike many other predictions, this one was made before the turbine was installed. The prototype was commissioned later, and it was stable up to maximum load [31].

As explained in Sect. 1.5 and in [32], the concept of using the downstream flow q_2 as a reference for mass flow gain χ in draft tube flow usually requires much lower magnitude of χ for instability compared to the use of q_1; therefore it overestimates in a systematic manner the destabilizing effect. To close further speculation about the correct approach, a study was conducted in 2009 to directly compute the unsteady behavior of a cavitating, rotationally symmetric vortex [33]. It was confirmed that two-phase computation is indispensable.

As shown in Fig. 2.9, taken from the study [33], the vortex shape resulting from the two-phase model has features known from physical model tests that cannot be reproduced by a single-phase computation. In case of large cavities, it shows a characteristic annular hydraulic jump and an undular structure reminiscent of standing waves.

The transient two-phase computations required a very high spatial resolution. Oscillation of the vortex flow was forced by means of a prescribed time-dependent variation of the draft tube intake velocity field. The response of the draft tube intake pressure, cavity volume, and draft tube exit discharge were simulated for transients with different forcing frequency. The structure and parameter values of a frequency-domain model for the dynamic transmission behavior of the full-load vortex were then identified. A large fraction κ of the mass flow gain effect depends on the runner exit flow q_1 (red curve in Fig. 2.10). The dead time t_d mentioned in

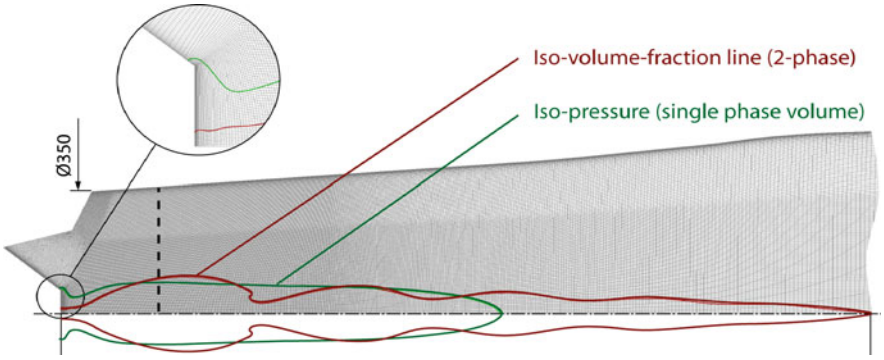

Fig. 2.9 Cavity contour obtained from single-phase and two-phase CFD model

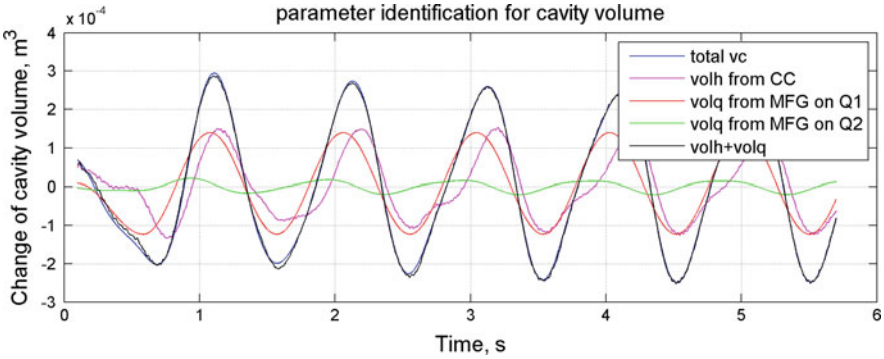

Fig. 2.10 Synthesis of cavity volume in identification procedure

Sect. 1.5 is essential. A small portion $1 - \kappa$ of the mass flow gain effect (between 0 and 4 %) was found to apply to the downstream side; it has only a minor influence on stability (green curve). The resulting lumped parameter model [33] for the cavity volume is

$$V_c = -C_C \cdot p_c - \chi \cdot (\kappa \cdot q_1(t - t_d) + (1 - \kappa) \cdot q_2) \tag{2.5}$$

Self-excited pulsation at full load has in a number of cases been successfully reduced by air admission to the draft tube center, preferably through the shaft [34, 35], see also Sect. 8.2]. Draft tube fins, which are described below, are not effective because, other than in partial load, at high load the main flow is not concentrated at higher radius.

2.2.8 Full-Load Vortex: Forced Oscillation

In some turbines the helical vortex shape also prevails at full load. It is probably associated with low axial flow velocity in the hub region and can therefore usually be avoided by appropriate runner design. The corkscrew vortex at full load has therefore become quite seldom in modern turbines. There is also an influence of the cavitation number. The corkscrew shape may exist at rather high cavitation number but disappear when the size of the cavitating core increases due to lower pressure. A similar behavior is also known with respect to the partial-load vortex, but due to stronger diffuser effect in the draft tube it is much more important at high load.

The physical properties of the forced full-load surge are similar to the half-load surge. The main difference is that, due to the higher level of flow velocity at comparable swirl number, the frequency is higher than at part load. In a well-documented historical case (reported in Sect. 8.1) the helical shape was observed in the model test, and the DTPP could be measured both at plant sigma and in absence of cavitation. For the successful countermeasure, see Sect. 8.1. In this problem, draft tube fins have also been found ineffective.

2.2.9 System Response

Pressure pulsation in the draft tube is the most common effect caused by the draft tube swirl. Quantitative data may be found in Sect. 7.2.1, some explanations of the hydraulic system response in Sect. 7.2.1 The so-called synchronous part of draft tube pulsation is associated with upstream (i.e., penstock) pressure pulsation, and this in turn can only be produced if the turbine discharge pulsates. The pulsation of turbine discharge (and head), power swing, and in some cases axial vibration (runner, shaft, generator support bracket), are all related to the 'synchronous' pulsation. On the other hand, radial vibration (runner shaft and bearing housing), and some of the low-frequency components of draft tube wall vibration are related to the 'asynchronous' part.

2.2.10 Mechanical Effects

Runner stresses caused by the partial-load vortex have been studied by on-board measurements [36]. A result including the vortex rope effect is shown in Fig. 1.15 in Sect. 1.6.

Although the draft tube rope may not have important effects on the runner [37, 38], long-term operation under rope condition may have more important effects on the draft tube components (cone, door, liner, pier, concrete) as shown in

Fig. 2.11 Crack in concrete at draft tube door

Fig. 2.12 Crack at junction of discharge ring to draft tube liner

Figs. 2.11 and 2.12 for machines operated for extended period of time at low-load conditions.

The asymmetric pressure distribution created by the helical vortex at partial load also acts on the runner. This asymmetry results in a rotating radial force and bending torque acting so that the runner performs a lateral vibration whose frequency, seen from the stationary system (casing, bearings) is the precession frequency of the vortex. This rotating radial force, which may also be observed and measured in model tests (see [39] and Sect. 7.3.3), creates a characteristic feature in the vibration behavior of the Francis turbines, shown in Fig. 2.13 for a pump turbine. The shaft vibration also shows a discontinuous change at the lower limit of vortex stability, in a similar way to the DTPP signals.

The ISO 7919 vibration standard [40] excludes pump turbines, but for Francis turbines the limits required by the standard are sometimes difficult to fulfill. For a

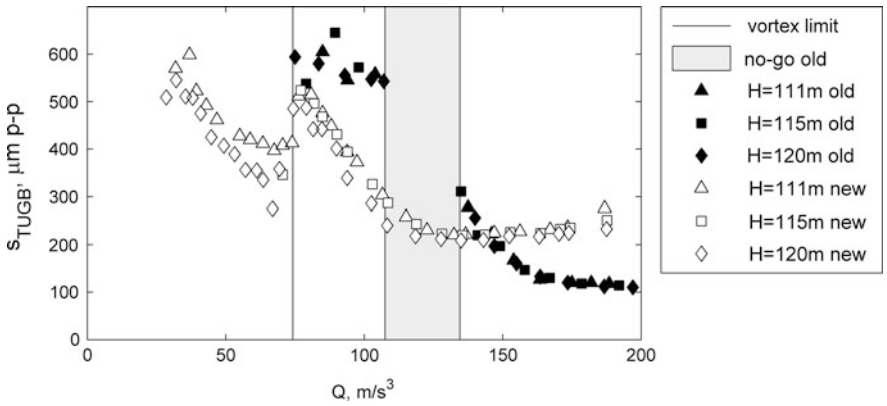

Fig. 2.13 Radial shaft vibration of a pump turbine

machine with the same synchronous speed as the one in Fig. 2.13 (166.7 rpm), the peak-to-peak amplitude of shaft vibration would not be allowed to exceed 250 µm. As the standard does not distinguish between turbine types that develop a part-load vortex (Francis, pump turbines, fixed-blade propeller) and machines that do not (Kaplan, Pelton), it is obvious that the Francis turbines are more critical with regard to fulfillment of vibration standard. Figure 2.13 also shows that even in case of refurbishment, where the draft tube remains the same, the quality of runner exit flow has an important influence on shaft vibration. The black markers in the figure show the behavior of the original runner that could not operate safely in the 'forbidden range' indicated as 'no-go old.' The replacement runner reduced the maximum vibration and eliminated the operational restriction.

In some cases it is likely that flow disturbances connected with the draft tube vortex have excited penstock vibration. Klein et al. [41] reported a case where intense vibration of the penstock shell occurred in the upper partial-load range, at approximately f/n = 1.33. The cure to this problem, likely caused by side effects of the part-load rope (Sect. 2.2.6), was to add stiffener rings to the penstock; the hydraulic cause was apparently not attacked.

In another case [42] the penstock vibration was caused by high-load surge with f/n ≅ 0.30, and was mitigated by air injection.

2.2.11 Peculiarities of Francis and Other Turbine Types

The draft tube shape has an important influence of draft tube surging. In early years, the US Bureau of Reclamation [2] even performed research using only the draft tube and no runner but with a swirl generating apparatus. Today, it is clear that the runner is essential for such tests, which makes it useful to compare replacement runners from different suppliers in comparative model tests. It is

known from many rehabilitation projects that a good runner outlet velocity profile may bring significantly better smoothness of operation (see Fig. 2.13 for an example).

2.2.11.1 Shallow Draft Tubes

In turbines with very shallow draft tubes there is often a small radius of curvature radius on the inner side of the elbow. In such cases the part-load vortex comes very close to the elbow contour in every revolution. As a consequence such draft tubes may give rise to high local amplitudes.

2.2.11.2 Straight Conical Draft Tubes

Conical draft tubes are a special case because in the absence of an elbow there is no forced oscillation excited by the usual mechanism. In these machines there is only the asynchronous pulsation. In practice, such turbines can also cause problems. In a turbine with a horizontal axis the vortex precession going through zones of different elevation can still cause periodically variable cavitation and provoke a small synchronous pulsation, in this case of a parameter-excited type. Also, the straight horizontal draft tube hardly responds to aeration because no air is retained in the vortex. By contrast, aeration in turbines with vertical axis is more effective because the air cannot escape easily.

2.2.11.3 Pump Turbines

Draft tube surge in pump turbines is of minor practical importance because pump turbines are designed to frequently pass through transients with much higher pulsation and vibration compared to the part-load surge. Because of this and the higher draft tube pressure level, aeration is seldom necessary. Draft tube surge may nevertheless cause problems if the machine is connected to a long tailrace. In such a case, the high water inertia combined with the small draft tube cavitation compliance may become critical for resonance. For a case example, see [43].

Draft tube inserts such as fins are seldom used, partly because there is a risk of runner damage in pump operation if an insert should fall off. An interesting application has been described in [44]. Model test results from pump-turbine models are shown and discussed in Sect. 7.3.1

2.2.11.4 Kaplan Turbines

In ordinary (double-regulated) Kaplan turbines, draft tube surge is also less important. The available range of runner blade angle adjustment, as defined by the

servomotor, is usually selected in a way as to permit on-cam operation in the foreseen load range. If running on-cam, the turbine produces too little runner exit swirl for a surge. Turbines operating off cam, due to very low load, or fixed-blade propeller turbines, have swirl properties comparable to Francis turbines. A survey of vortex phenomena for various loads has been given by Skotak and Pulpitel [45]. For model test results, see Sect. 7.4

In transient operation however, draft tube surge occurs in every Kaplan turbine. If the unit rejects load, then it has to pass through conditions with large residual swirl; at the instant of maximum speed, the runner torque is zero and the whole swirl generated in the wicket gate is passed through into the draft tube. For that reason large pressure fluctuations at vortex frequency may occur in the draft tube. Sometimes they may give rise to pressure shocks because also the amount of vortex cavitation becomes quite considerable. This is partly due to the deceleration of discharge while the guide vanes are closing. Typically, the resulting pulsation has a frequency of the order of 1 Hz, and fortunately only a few cycles. In some cases it may be necessary to improve the behavior by choosing a more suitable maneuver of the runner blades and wicket gate during load rejection.

2.2.11.5 Valves and Gates

Shutoff devices located downstream of a Francis turbine or pump turbine may also be affected by the draft tube vortex. The precession movement of the vortex continues even downstream of the draft tube elbow. Valves or gates in this environment must be secured absolutely reliably. A singular case has been reported [46] where a spherical valve at the end the draft tube of a high-head Francis turbine started to swing due to the draft tube vortex but was secured in time. Closure of such a valve during turbine operation would entail headwater pressure in the draft tube, with catastrophic consequences.

2.2.12 Prediction and Assessment

Until today, the most reliable source of information about the dynamic behavior of a turbine prior to construction is still the laboratory test with a reduced-scale model. The most important unsteady flow and pressure patterns like the part-load vortex or inter blade vortices may be taken as similar representation of prototype behavior, as far as their local consequences in the draft tube are regarded.

Dynamic similarity is never perfect because many kinds of oscillation phenomena have a global component that depends on system response [47], namely, the water conduit of the installation (test rig, or power plant) and the rotating assembly connected with the runner (brake, generator plus grid). These components of the pulsation may be subject to important distortion, as cautioned in the

IEC 60193 standard. The 'synchronous' component of the ordinary part-load oscillation is a good example [3].

Apart from the system dependency, the representation of cavitation may also cause deviations from similarity. Due to the large draft tube depth in vertical-axis turbines, the gravity component of the pressure distribution has an important influence on the vortex behavior. To correctly represent this influence, the condition of equal Froude number should be fulfilled together with the Thoma cavitation number σ. Equal Froude number means that the ratio between prototype head and model test head should be equal to the geometric scale:

$$\mathrm{H}_M/\mathrm{H}_P = \mathrm{D}_M/\mathrm{D}_P \tag{2.6}$$

In model tests for very large prototypes, this condition results in very high suction head which can often not be realized at the test rig; in such cases the natural frequency of the draft tube cannot be expected to correspond to prototype. For that reason, hydraulic resonance conditions may be shifted to a different load condition or σ value.

The common sense approach to model-based prediction, also incorporated in the standard (Sect. 4.3.7 of [25]), is to expect the frequencies to transform proportional to the runner

$$\mathrm{f}_M/\mathrm{f}_p = \mathrm{n}_M/\mathrm{n}_p \tag{2.7}$$

and the pulsation amplitudes proportional to the net head (or energy)

$$\tilde{p}_M/\tilde{p}_P = E_M/E_P \tag{2.8}$$

Accordingly, it is common practice to use relative frequencies f/n and relative amplitudes (pressure factor $\tilde{p}_E = \tilde{p}/\rho E$) to characterize the pulsation test results. Other concepts, better adapted to the physical phenomena, have been suggested by the standard ([25], in particular par. 4.3.7.3), and by some authors [11, 48, 49], but apparently have not been adopted in practice. For a discussion, see [32].

Putting aside the issues of transferability, another important question is the admissible amount of pulsation. This matter has not been regulated by an international standard, and it seems that quantitative data have not been published by anybody since the 1980 s. Unrealistic ideas are therefore quite often encountered in technical specifications. One of the goals of this handbook is to provide information to counter this shortcoming. A very simple, unscientific, and yet quite practical limit for a prototype Francis DTPP would be

$$\Delta\mathrm{h}_{\mathrm{p-p}} < \mathrm{sqrt}(\mathrm{H}_\mathrm{r}) \tag{2.9}$$

wherein $\Delta\mathrm{h}_{\mathrm{p-p}}$ is the maximum peak–peak amplitude (97 % confidence level) anywhere at the draft tube wall, and H_r is the rated head of the turbine, both figures in mwc at the prototype.

A more sophisticated, and 'scientifically acceptable' limit would be the generic curve presented in Sect. 7.2.1, Figs. 7.7 and 7.9. The authors recommend to no

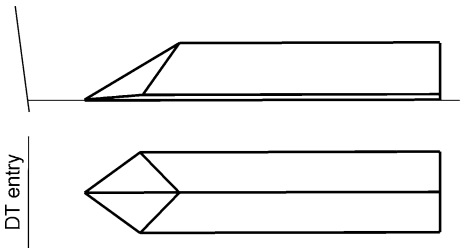

Fig. 2.14 Draft tube fin shape

longer define guarantees as constant pressure factor for different values of operating head but as absolute values for pressure pulsation for physical reasons: As the turbine has the same speed and the same draft tube at minimum and maximum head, and as the draft tube vortex does not significantly depend on head, it will also have the same absolute draft tube pulsation.

2.2.13 Countermeasures

In the different types of draft tube surges (Sects. 2.2.1–2.2.8), different physical phenomena are involved. There is no single countermeasure suitable for all types of problems. For instance, draft tube fins are almost certainly useless if the problem is high-load surge.

Therefore, countermeasures have been mentioned as suitable in the pertinent chapters.

2.2.13.1 Draft Tube Fins

Draft tube fins [50, 51] are often a solution to problems caused by the part-load vortex. Depending on the draft tube profile, fins with different proportions have proven effective. Figure 2.14 is a shape that can be successfully used in many draft tube contours. Four fins to be set at 45° against the draft tube symmetry plane. The use of fins requires some caution, see Sects. 2.4.3.

The main effect of draft tube fins on the part-load pulsation is to reduce the amplitude of the pressure source Δp_{EX}, and therefore also the synchronous pulsation. Accordingly, it is the method of choice for suppressing cavitation-related draft tube resonance as well as power swings. Using the analytical procedure described in Sects. 2.2.1, the forcing term Δp_{EX} has been evaluated for a medium-head turbine. As shown on the left-hand side of Fig. 2.15, the excitation is almost completely eliminated. There is less influence on the asynchronous component (not shown). At the same time, the precession frequency is somewhat increased, typically by 10–15 %. As already mentioned, fins are usually ineffective with regard to problems at high load, i.e. flow rates higher than the swirl-free discharge.

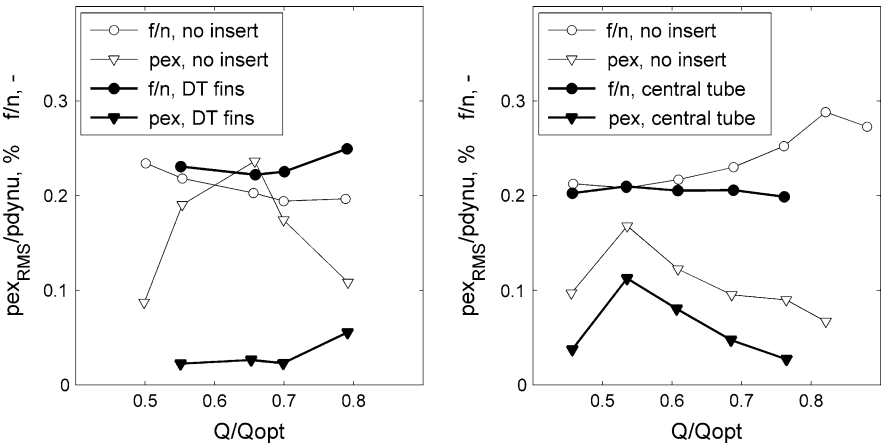

Fig. 2.15 Effect of draft tube inserts on part-load pulsation parameters. **a** $n_{QE} = 0.18$, draft tube fins. **b** $n_{QE} = 0.23$, central column

2.2.13.2 Draft Tube with a Central Column

Draft tube surges can also be reduced by means of other types of draft tube inserts. Placing a central tube in the draft tube axis, between the runner hub and elbow, may also provide smoother operation [52]. This design was probably inspired by the much older Moody cone. As shown on the right-hand side of Fig. 2.15, it also has some effect on the pressure source. The indicated frequency is the precession frequency. For the three test points with $Q/Q_{opt} \leq 0.63$, the vortex has two threads (see Sects. 2.2.3), therefore the actually measured frequency of pressure pulsation for these points was twice the value indicated in the plot. It is likely that this type of insert is also useful for stabilization at high load, however, no reliable results seem to be available.

There is a considerable lateral force of the vortex rope acting on the central tube; therefore sufficient radial support is essential. Stress concentrations at locations where radial struts join the draft tube wall and central tube are possible problem areas to be considered.

2.2.13.3 Air Admission

Air admission or air injection is very often beneficial [53, 56] because it smoothes out the annoying high-frequency components of noise and vibration. In addition, aeration sometimes removes flow instability by manipulating the hydraulic transmission behavior—in particular lowering the draft tube natural frequency. This effect can also be counterproductive in certain cases because a resonance of the synchronous draft tube pulsation may be produced by air injection in a pump-turbine or Francis turbine with rather high submergence.

Little has been published about the effect of flow aeration on turbine efficiency. Losses due to aeration increase with the relative air flow rate. Information about efficiency losses due to aeration has sometimes been collected in connection with tests aiming at increased tail water oxygen content [54, 55].

Depending on design, it is often necessary to add inserts in the draft tube, like tripods or pipes protruding from the draft tube wall. These structures obstruct the flow and cause additional drop in efficiency. Such additional loss may be avoided if air can be admitted through the shaft bore or head cover.

The turbine axis is, because of the radial pressure gradient due to swirling flow, the most suitable location for draft tube aeration by means of atmospheric air. In many cases air can be admitted through the hollow turbine shaft. Self-aspirating aeration may become more difficult or impossible if such an air path is not foreseen. Possible solutions depend on the design applied for axial thrust compensation. Solutions for turbines with external balancing pipes are shown in [56] and in Sect. 8.2 An example for a turbine with axial thrust compensation using a baffle plate is described in [57].

The effect of draft tube aeration on DTPP is often tested during reduced-scale model tests. Such a test demonstrates the possible effects in a purely qualitative manner. Quantitative data, like relative air rate, efficiency drop, or reduction of pulsation amplitude, must not be expected to be transferable.

2.3 Runner Inter Blade Vortex

2.3.1 Physical Mechanism

At part load the flow angle at runner inlet is no more optimally aligned with the blade inlet angle. High incidence occurs especially near hub and shroud which leads to a vortex which is driven through the blade channel toward the runner outlet.

2.3.2 Prediction, Features, Diagnosis

The inter blade vortex phenomenon is amenable to visual observation in the course of a model test, this holds at least in its well-developed form, see also Fig. 5.1.

2.3.2.1 Numerical Simulation

As the flow phenomenon of the inter blade vortices requires extremely high grid resolution (20 grid cells to resolve the vortex core), standard CFD simulations in industry usually reveal inter blade vortices in a coarse way only. There is an

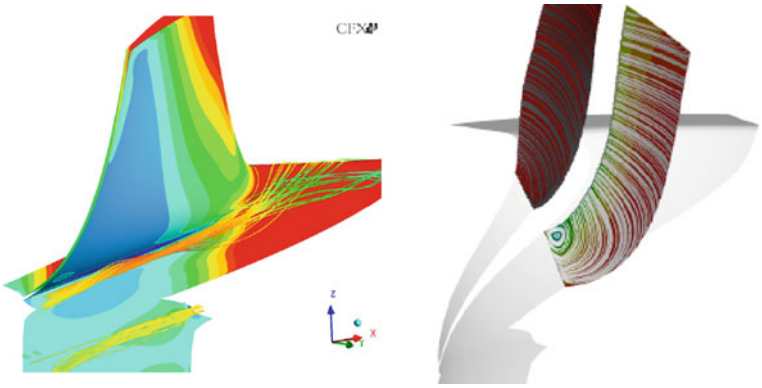

Fig. 2.16 CFD simulation of the inter blade vortex (ANDRITZ internal research, 2008)

example of a CFD simulation published by Stein et al. [14], of inter blade vortices occurring at part load. Another example is given in Fig. 2.16. In the cut-away view on the left-hand side the formation of the inter blade vortex from streamlines originating along the band-side runner entrance is visualized. The streamlines indicating the vortex are colored by velocity magnitude (red: high velocity, green: low velocity).The right-hand side shows the result of a CFD simulation of the inter blade vortex in a Francis runner. The distribution of static pressure on the blade and shroud is also shown from red (high pressure) to blue (low pressure). On the right-hand side the secondary flow patterns in the blade channel are illustrated by lines of the absolute velocity in a cross section showing clearly the center of the inter blade vortex.

To the author's knowledge no attempts have been made so far to predict time-dependent aspects of these vortices.

2.3.3 Operation Range Affected

Typical areas in the turbine hill chart are indicated in Fig. 5.1 (Sect. 5.2—discharge too low/head too high). The limits d and e may combine to form a single limit. Limits f and g in that figure are corresponding phenomena if the incident flow to the runner blades is wrong in the opposite sense (discharge too high/head too low). The example shown below in Fig. 2.18 belongs to the latter category.

2.3.4 Detrimental Effects

Pressure pulsation due to inter blade vortices is of an irregular wide-band nature and may be quite intense. It is not easy to quantify due to its stochastic, wide-band

Fig. 2.17 Cavitation erosion caused by inter blade vortex

nature. In a Francis turbine with 2.4 m runner diameter, rated 56 MW at 300 rpm, it was found that maximum intensity at the runner occurred at a higher frequency (about 250 Hz) compared to the turbine intake (about 50 Hz). Both values correspond to a Strouhal number—using the width of the runner blade channel at the runner intake and exit, and the pertinent relative velocity—in the range of 0.5–1.0; however it is not clear if these values are typical.

Inter blade vortices are known to create cavitation in runner blades flow channels, at the crown and sometimes also at the blades (see Sect. 5.3 on cavitation). Accordingly, considerable damage by erosion may result in some cases. An example for erosion by inter blade vortex (in this case due to excessive high discharge at low head) is shown in Fig. 2.17, another one in Fig. 5.3.

Strong mechanical vibration may be caused by cavitation because the wide-band excitation spectrum may excite the natural frequencies of many components of the turbine structure. It is also possible that pressure pulsations travel upstream into an exposed penstock and cause alarming shell vibration. In one plant, penstock vibrations (Fig. 2.18) near the upstream valve downstream of the surge tank, were clearly caused by pressure pulsation due to vortex cavitation in the runner. This could be proven beyond doubt because the pressure signals at the valve house, upstream (p5) and downstream (p6) of the safety butterfly valve were sufficiently coherent for several bands of frequency. The phase shift between the pressures was proportional to frequency, and corresponded to a plausible figure of wave speed. The distance of sensor locations $\Delta L = 7.54$ m and phase shift of 180 dg (half wavelength) at 58 Hz, together with the definition of wavelength ($\lambda = a/f$), yields a wave speed of $a = 2 \times \Delta L/f = 875$ m/s. This is also an example for a simple and reliable way of diagnosis, clearly indicating that the pressure waves are arriving from a source downstream (in this case as far as 350 m downstream) of the point of interest. It is also interesting that no coherence existed between the pressure and vibration velocity signal, yet there could be no doubt that the pressure pulsation excites the shell vibration.

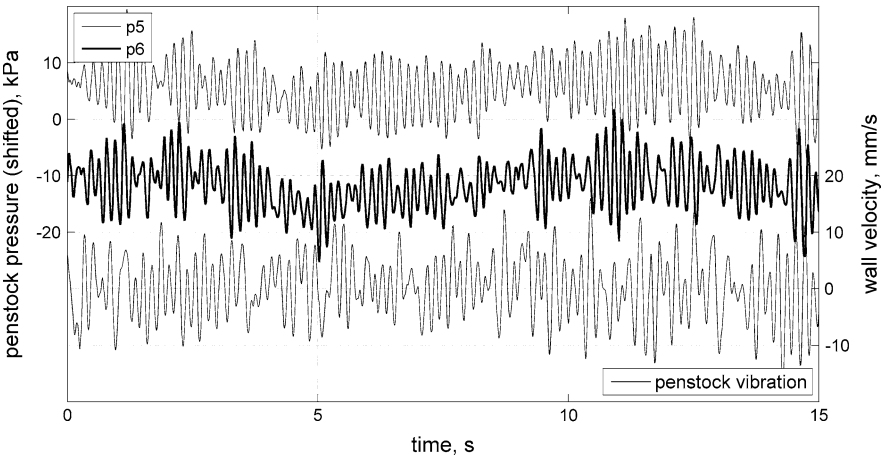

Fig. 2.18 Penstock shell vibration excited by runner cavitation

2.3.5 Countermeasures

To some extent, the limits of occurrence can be pushed back by adequate layout of the runner blade profile. If the range of operating heads in a Francis turbine is extreme, the occurrence of inter blade vortex at partial load and high head may become unavoidable.

As an example, in a large plant the maximum head is 2.6 times higher than the minimum head. At very high head—about 125 % of best efficiency head—the operation becomes very rough and extremely noisy. In such a case, air injection upstream of the runner is often highly effective in vibration and noise abatement. In the above-mentioned example air is supplied through a circular manifold above the head cover, connecting to a set of flush air intake holes, one downstream of every guide vane. In this example, the reduction in noise level due to air injection is −8 dB, a remarkable improvement.

An early description of upstream aeration for a low-head Francis turbine has been given by Malamet [58]. In some projects, air injection upstream or inside the runner has also been applied to reduce the erosion rate in runners of water turbines and storage pumps.

2.4 Vortex Breakdown: Other Locations

2.4.1 Penstock Manifold

Forceful vortex breakdown phenomena may take place in quite unexpected environment. In a medium-head power plant, the inflow was distributed to the

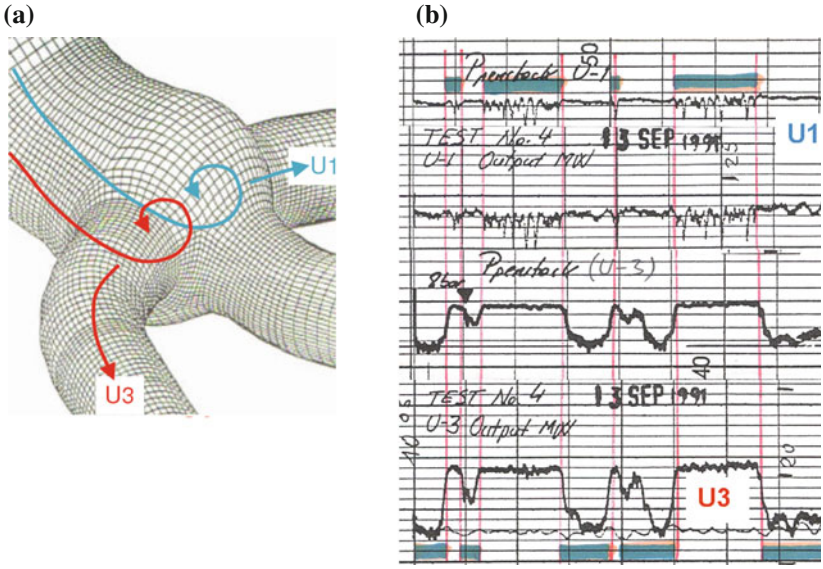

Fig. 2.19 Vortex breakdown in a penstock manifold. **a** Trifurcation with vortex. **b** Pressure and power dropouts

three turbines by a manifold. The manifold was a trifurcation built with a spherical body from which the three branches were fed (Fig. 2.19, left-hand side). The penstock entered the sphere with considerable eccentricity, the lateral branches are connected at an inclination of approximately 70 dg. The design successfully passed standard steady-state performance tests in a hydraulic laboratory, whereby no anomalous behavior was noticed.

A strange problem was detected when plant operation with all three turbines started. Every now and then, the output of unit 3 dropped by as much as 20 % and continued at the reduced level for a few minutes, then recovered to normal. Similar dropout occurred at unit 1 but not at unit 2. Recordings of power and turbine intake pressure of the units (Fig. 2.19, right-hand side) showed that the power variations were caused by a corresponding variation of turbine intake pressure, which in turn needed to be explained.

A closer look into the recordings reveals that the dropout periods at units 1 and 3 are mutually exclusive, as indicated by the green bars in the record. Some phenomenon makes the trifurcation act as a kind of fluidic switch that alternately throttles the inflow to the two lateral branches. The mechanism is comparable to the one acting in a flow device (‘vortex throttle’) used for one-way throttling in some surge tanks. The very eccentric inflow from the penstock to the spherical chamber obviously produces a strong rotational flow in the sphere with horizontal axis. Entering the side branch, this swirling flow is forced into a much smaller radius, with corresponding increase of tangential velocity. The vortex breakdown in the side branch creates a substantial pressure loss at the turbine intake. The flow

in the sphere is asymmetric. The throttling effect occurs at one lateral branch at a time, while the opposite branch recovers, and vice versa.

Later this problem has been studied by detailed laboratory tests as well as CFD simulations [59]. It was finally cured by inserting a 'roof' plate into the sphere which effectively inhibited the formation of vortices [60].

2.4.2 Kaplan Hub

As an initial step toward understanding the instability phenomena of swirling flows, engineers in the 1930s investigated the disintegration of a concentric pipe flow [1]; it was then that the dead water core was discovered. Later, Eichler [61] made use of this formalism to explain a flow disturbance occurring in axial turbines. A dead water core may form upstream of the runner of a Kaplan or bulb turbine when operating with a small guide vane opening. In the shear zone between this dead water core and the main flow, there are often strong spiraling vortex filaments. The appearance is somewhat similar to a draft tube vortex but there are usual several filaments at the same time. In some turbines there may be one vortex per runner blade that may extend downstream through the runner. In general, dead water core diameter is a function of the wicket gate opening but the intensity is a function of discharge, the phenomena getting stronger at large runner opening.

Pulpitel [62] found between one and four filaments traveling around the hub. He studied critical combinations of the number and precession frequency of those vortices both in a model and the pertinent large prototype of a four-blade Kaplan turbine. Under certain circumstances, the vortices may produce rotor whirling with large lateral shaft displacement. The criterion for an excitation of ν cycles (node diameters, see also Sect. 3.1) around the runner circumference is[3]

$$\nu = k \times Z_r - m \times Z_D \tag{2.10}$$

where k and m are low integers and

Z_r = number of runner blades
Z_D = number of disturbances (i.e., vortex filaments).

A whirling movement of the runner is excited if $\nu = \pm 1$, and the frequency f_s seen in the stationary system (bearings, casing), in the most important case $m = k = 1$ is

$$f_s = Z_r \times n - Z_D \times f_0 \tag{2.11}$$

n = runner rotation frequency
f_0 = precession frequency of the vortex flow field.

[3] Compared to [62], the definitions have been adjusted to comply with Sect. 3.1.

There were quite frequently $Z_D = 3$ vortices rotating at about 60 % of runner speed, thus the four-blade runner was subject to whirling at roughly 2.2 times runner speed.

A typical operational situation where these phenomena become important, is the sluicing maneuver. During sluicing, the turbine is disconnected from the grid but has to discharge as much water as possible. Accordingly, the runner blades are wide open but the wicket gate must be partially closed in order to limit the speed. A peculiarity of the sluicing operation is that the entire swirl produced by the wicket gate is passing through the runner and draft tube. The draft tube flow is therefore also potentially unstable.

2.4.2.1 Numerical Simulation

Similar to the case of the inter blade vortices, the vortices around the Kaplan hub require extremely high grid resolution in order to resolve the vortex cores with 20 grid cells each. Such computational grids are at the limit of today's industrial standard. Nevertheless, an internal CFD study was carried in 2004 out by ANDRITZ Hydro with relatively high grid resolution in order to better understand the flow mechanisms acting near the hub at low part load (30 % of optimum load), see figure. A structured hexahedral computational grid was used with second order accurate spatial discretization. Several operating points were simulated in order to be able to unambiguously identify the cause for the pressure pulsations observed at extreme part load.

At flow rates of 60 % and higher, no vortex structure could be identified between guide vanes and runner blades but at 30 % load strong vortex structures were found near the runner hub. The Fig. 2.20 displays the geometrical proportions of the studied turbine (a) and a simulation result of the flow pattern between guide vanes and runner blades (b).

2.4.3 Draft Tube Fin Tip Vortex

Draft tube fins are often used in Francis turbines because they are a reliable countermeasure against the surge at partial load. If not properly used, they may however cause collateral damage. At reduced discharge, the draft tube flow meets the fins at a considerable angle of attack, giving rise to a secondary vortex starting at the leading edge of every fin, as shown in Fig. 2.21 for a medium-head Francis turbine. In the figure, the appearance of the secondary vortex at one out of four fins, as seen by the test engineer, is shown for various conditions of turbine load, i.e., draft tube swirl.

Cavitation is usually present in the core of the vortices, depending on the runner exit swirl. This measure can therefore produce unwelcome secondary pressure fluctuation at higher frequency, counteracting the desired reduction of pressure

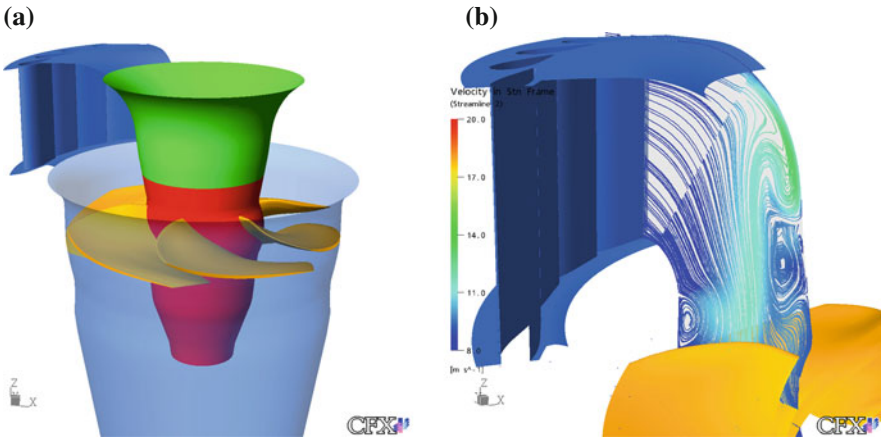

Fig. 2.20 CFD simulation of vortex structure near the Kaplan runner hub. **a** Geometry of the Kaplan runner. **b** Vortex structure at the hub

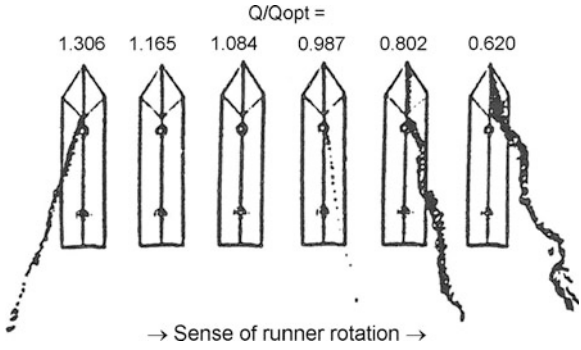

Fig. 2.21 Draft tube fin tip vortex observed at plant sigma, $n_{QE} = 0.146$

pulsation. In addition, the cavitating tails of the vortices often hit the draft tube wall that, as a consequence, has to be protected against cavitation. Such protection can be made by welding erosion-resistant plates to the draft tube wall in the wake region of the fin.

There is also a more effective means of protection. In case of substantial swirl, the leeward side of the fin tip normally has a small area of very low pressure. By providing a small hole at each one of the fins and connecting the holes to a manifold, it is normally possible to introduce atmospheric air by natural suction [44, 50]. No further protection of the wall is required and, equally important, the parasitic pressure fluctuations are also eliminated. The two references provide some quantitative information concerning the suction effect available at the fins. For more detailed data from ANDRITZ model tests, see Sect. 7.2.2.

References

1. Meldau, E. (1935). *Swirling flow in rotationally symmetric cavity* (in German). PhD thesis, Technical University Hannover.
2. Cassidy, J. J., & Falvey, H. T. (1970). *Frequency and amplitude of pressure surges generated by swirling flows.* IAHR Section Hydraulic Machinery, Equipment, and Cavitation, 5th Symposium (Stockholm, 1970), paper E1.
3. Nishi, M., Kubota, T., Matsunaga, S., & Senoo, Y. (1980). *Study on swirl flow and surge in an elbow type draft tube*. IAHR Section Hydraulic Machinery, Equipment, and Cavitation, 10th Symposium (Tokyo, 1980), Vol. 1, pp. 557–568.
4. Nishi, M., Kubota, T., Matsunaga, S., & Senoo, Y. (1984). *Surging characteristics of conical and elbow-type draft tubes*. IAHR Section Hydraulic Machinery, Equipment, and Cavitation, 12th Symposium (Stirling, 1984), pp. 272–283.
5. Rheingans, W. J. (1940). Power swings in hydroelectric power plants. *Transactions of the ASME, 62*, 171–184.
6. Ulith, P., Jaeger, E. U., & Strscheletzky, M. (1974). *Contribution to clarifying the inception of nonstationary phenomena in the draft tube of high specific speed Francis turbines operating at part load*. IAHR Section Hydraulic Machinery, Equipment, and Cavitation, 7th Symposium (Vienna, 1974), paper III-4.
7. Moody, L. F. discussion of [1].
8. Brennen, C. (1978). *The unsteady, dynamic characterization of hydraulic systems with emphasis on cavitation and turbomachines.* Joint ASME/ASCE/IAHR Symposium, Fort Collins, 1978, pp. 97–107.
9. Dériaz, P. (1960). *A contribution to the understanding of flow in the draft tubes of Francis turbines*. IAHR Section Hydraulic Machinery, Equipment, and Cavitation, 1st Symposium (Nice, 1960), paper B-1.
10. Doerfler, P. (1982). *System oscillations excited by the Francis turbine's part load vortex core: Mathematical modelling and experimental verification* (German text, English summary). Dissertation, Technical University Vienna (Austria), October 1982.
11. Doerfler, P. (1982). *System dynamics of the Francis Turbine Half Load Surge*. IAHR Section Hydraulic Machinery, Equipment, and Cavitation, 11th Symposium (Amsterdam, 1982), Vol. 2, Paper 39.
12. Ruprecht, A., Helmrich, Th., Aschenbrenner, Th., & Scherer, Th. (2001). *Simulation of pressure surge in a hydro power plant caused by an elbow draft tube.* 10th International Meeting of the work group on the behaviour of hydraulic machinery under steady oscillatory condition, Trondheim, Norway.
13. Sick, M., Dörfler, P., Lohmberg, A., & Casey, M. (2002). *Numerical simulations of vortical flows in draft tubes.* WCCM V, Vienna, Austria, 2002.
14. Stein, P., Sick M., Doerfler P., White, P., & Braune, A. (2006). *Numerical simulation of the cavitating draft tube vortex in a Francis turbine*. IAHR Section Hydraulic Machinery, Equipment, and Cavitation, 23rd Symposium, Yokohama, Japan, 2006.
15. Wahl, T. L., Skinner, M. M., Falvey, H. T. (1991). *The Twin Vortex Draft Tube Surge.* Waterpower'91, pp. 2011–2020.
16. Dörfler, P., Bloch, R., Mayr, W., & Hasler, O. (1988). *Vibration tests on a high-head (740 m) Francis turbine: Field tests from Häusling.* IAHR Section Hydraulic Machinery, Equipment, and Cavitation, 14th Symposium (Trondheim, 1988), Vol. 2, Paper D1.
17. Guarga, R., Hiriart, G., Torres, J. J. (1983). *Oscillatory problems at Mexico's La Angostura plant.* Water Power & Dam Construction, October 1983, pp. 33–36.
18. Glattfelder, A. H., Grein, H., & Huser, L. (1980). Self-excited oscillations in a hydroelectric unit. IAHR/IUTAM Symposium, Karlsruhe, 1979, Paper B11. In E. Naudascher & D. Rockwell (Ed.), *Practical experiences with flow-induced vibrations*. Berlin: Springer.
19. Gummer, J. H. (2007). Penstock resonance resulting from unstable turbine characteristics, Paper 21.01, Hydro 2007, Granada.

20. Doerfler, P. (1994). *Observation of pressure pulsations at high partial load on a Francis model turbine with high specific speed.* IAHR Work Group WG1 (The Behaviour of Hydraulic Machinery under Steady Oscillatory Conditions) 6th Meeting, Lausanne 1993, also in: Hydro-power & Dams, January 1994.
21. Billdal, J. T., & Holt, B. G. (2000). *Three Gorges project: Review of GE energy Norway's hydraulic design*. Proceedings of the Hydraulic Machinery and Systems 20th IAHR Symposium (Charlotte, 2000).
22. Shi, Q. (2008). *Experimental investigation of upper part load pressure pulsations for Three Gorges model turbine*. IAHR 24th Symposium on Hydraulic Machinery Systems, Foz do Iguassú, October 2008.
23. Arpe, J., & Avellan, F. (2002). *Pressure wall measurements in the whole draft tube: steady and unsteady analysis.* Proceedings of the 21st IAHR Symposium on Hydraulic Machinery and Systems, Lausanne, Switzerland, September 2002, pp. 593–602.
24. Rudolf, P., Pochyly, F., Hában, V., & Koutnik, J. (2007). *Collapse of cylindrical cavitating region and conditions for existence of elliptical form on cavitating vortex rope*. IAHR WG (Cavitation and Dynamic Problems in Hydraulic Machinery and Systems) 2nd Meeting, Timisoara Romania, October 24–26, 2007.
25. Nicolet, C., Zobeiri, A., Maruzewski, P., & Avellan, F. (2010). *On the upper part load vortex rope in Francis turbine: Experimental investigation.* 25th IAHR Symposium on Hydraulic Machinery and Cavitation, Timisoara 2010.
26. Kirschner, O., Ruprecht, A., & Göde, E. (2009). *Experimental investigation of pressure pulsation in a simplified draft tube, Proceedings of the 3rd Meeting IAHR Workgroup on Cavitation and Dynamic Problems in Hydraulic Machinery and Systems*, Brno 2009, Paper B1.
27. Strohmer, F. (1975). *Investigation of the operational behaviour of a Francis turbine with high specific speed below best efficiency point* (in German). Dissertation, Technical University Vienna (Austria), April 1975.
28. Fisher, R. K., Palde, U., & Ulith, P. (1980). *Comparison of draft tube surging of homologous scale models and prototype Francis turbines*. IAHR Section Hydraulic Machinery, Equipment, and Cavitation, 10th Symposium (Tokyo, 1980), Vol. 1, pp. 541–556.
29. Pulpitel, L. (1985). *Low frequency pressure oscillations in hydraulic systems with a pump turbine*. IAHR Work Group WG1 (The Behavior of Hydraulic Machinery under Steady Oscillatory Conditions) 2nd Meeting, Mexico City, 1985.
30. Flemming, F., Foust, J., Koutnik, J., & Fisher, R. K. (2008). *Overload surge investigation using CFD data.* IAHR 24th Symposium on Hydraulic Machinery Systems, Foz do Iguassú, October 2008.
31. Dörfler, P., Braun, O., & Sick, M. (2001). Hydraulic stability in high-load operation: a new model and its use in Francis turbine refurbishment. *Hydropower and Dams*, (4), 84–88.
32. Dörfler, P. K. (2009). *Evaluating 1D models for vortex-induced pulsation in Francis turbines. Proceedings of the 3rd Meeting IAHR Workgroup on Cavitation and Dynamic Problems in Hydraulic Machinery and Systems*, Brno 2009, Paper F3.
33. Dörfler, P. K., Keller, M., & Braun, O. (2010). *Full-load vortex dynamics identified by unsteady 2-phase CFD.* 25th IAHR Symposium on Hydraulic Machinery and Cavitation, Timisoara 2010.
34. Purdy, C. C. (1979). *Reducing power swings at Tarbela's turbines.* Water Power and Dam Construction, April 1979, pp. 23–27.
35. Arzola, F., Azuaje, Z., Zambrano, P., & Gulbrandsen, G. (2006). *Undesired power oscillations at high load in large Francis Turbines. Experimental study and solution*. IAHR Section Hydraulic Machinery, Equipment, and Cavitation, 23rd Symposium, Yokohama, Japan, 2006.
36. Lowys P. Y., Doyon J., Couston M., & Vuillerod G. (2001). *Dynamic behaviour of low head Francis turbines.* 10th International Meeting of the Work Group on the Behaviour of Hydraulic Machinery Under Steady Oscillatory Conditions, Trondheim, Norway, June 26–28, 2001.

37. Lowys P.-Y., Deniau J.-L., Gaudin E., Leroy P., Djatout M., (2006) On-Board Model Runner Dynamic Measurements, Hydrovision, Portland.
38. Coutu A., Monette C., Gagnon M., (2007) Life Assessment of Francis Runners Using Strain Gage Site Measurements, Waterpower XV, Chattanooga, TN, July 23-26, 2007.
39. Doerfler, P., Lohmberg, A., et al. (2003). *Investigation of pressure pulsation and runner forces in a single-stage reversible pump turbine model.* IAHR Work Group WG1 (The Behavior of Hydraulic Machinery under Steady Oscillatory Conditions) 11th Meeting, Stuttgart 2003.
40. ISO 7919 Mechanical vibration—Evaluation of machine vibration by measurements on rotating shafts Part 1: General guidelines Part 5: Machine sets in hydraulic power generating and pumping plants.
41. Klein, J., et al. (1976). *Investigation on vibrations of a large penstock, on the sources of their excitation and on getting them under control*. IAHR Section Hydraulic Machinery, Equipment, and Cavitation, 8th Symposium (Leningrad, 1976), paper I-3.
42. Gibberd, J. J. (1997). *Diagnosis and solution of severe hydro-mechanical vibrations following the upgrading of a 30 MW UK hydro station*. Conference on Refurbishment and Upgrading of Hydro Plants, October 1997, pp. 25–38.
43. Koutník, J., Nicolet, Ch., Schohl, G. A., & Avellan, F. (2006). *Overload event in a pumped-storage power plant.* IAHR Section Hydraulic Machinery, Equipment, and Cavitation, 23rd Symposium (Yokohama, 2006).
44. Pulpitel, L., Koutnik, J., & Skotak, A. (1998). *Natural air admission of a deep submerged pump turbine*. IAHR Work Group WG1 (The Behavior of Hydraulic Machinery under Steady Oscillatory Conditions) 9th Meeting, Brno 1999, paper A5, also in: Hydro Vision'98.
45. Skotak, A., & Pulpitel, L. (1997). *Behaviour of a Kaplan turbine model operating under off-cam conditions for a wide range of load*. IAHR Work Group WG1 (The Behavior of Hydraulic Machinery under Steady Oscillatory Conditions) 8th Meeting, Chatou 1997, paper G-1.
46. Wobornik, A. (1967). Observations downstream of Francis turbines with back pressure (in German). *EuM*, *84*(12), 488–493.
47. IEC 60193 Hydraulic turbines, storage pumps and pump-turbines—Model acceptance tests, Ed. 2.0, 1999–11.
48. Jacob, T., Prénat, J.-E. (1996). *Francis turbine surge: discussion and data base.* IAHR Section Hydraulic Machinery, Equipment, and Cavitation, 18th Symposium (Valencia, 1996), pp. 855–864.
49. Tadel, J., Maria, D. (1986). *Analysis of dynamic behaviour of a hydroelectric installation with a Francis turbine.* 5th International Conference on Pressure Surges, BHRA (Hannover, 1986), Paper G1, pp. 169–176.
50. Biela, V. (1998). *Draft tube fins*. IAHR Section on Hydraulic Machinery and Cavitation, 19th Symposium (Singapore, 1998), pp. 454–461.
51. Rocha, G., Sillos, A. (1982). *Power swing produced by hydropower units*. IAHR Section Hydraulic Machinery, Equipment, and Cavitation, 11th Symposium (Amsterdam, 1982), Vol. 2, Paper 44.
52. Lecher, W., Baumann, K. (1968). *Francis turbines at part-load with high back-pressure.* IAHR Section Hydraulic Machinery, Equipment, and Cavitation, 4th Symposium (Lausanne, 1968), Paper B-4.
53. Nakanishi, K., Ueda, T. (1964). Air supply into draft tube of Francis turbine. *Fuji Electric Review,* 10(3), pp. 81–91.
54. Harshbarger, E. D., March, P. A., Vigander, S. (1984). *The effect of hydro turbine air venting on generating efficiency, dissolved oxygen uptake, and turbine vibrations*. Tennessee Valley Authority, Water Systems Development Branch, Rept. WR28-1-600-107, March 1984.
55. Papillon, B., Sabourin, M., Couston, M., Deschênes, C. (2002). *Methods for air admission in hydroturbines.* 21th IAHR Symposium on Hydraulic Machinery and Systems, Lausanne, September 9–12, 2002.

56. Doerfler, P. (1986). *Design criteria for air admission systems in Francis turbines*. IAHR Section Hydraulic Machinery, Equipment, and Cavitation, 13th Symposium (Montreal, 1986), Vol. I, Paper 8.
57. Papillon, B., St.-Hilaire, A., Lindstrom, M., Sabourin, M. (2004). *Analysis of Francis head cover pressure and flow behavior inside runner cone.* Hydro Vision 2004, Montréal, QC, August 15–18, 2004.
58. Malamet, S. (1962). *Aeration of the turbines in the pumped storage plant Geesthacht* (in German). Elektrizitätswirtschaft 61, No. 8, 20-03-1962.
59. Ruprecht, A., Helmrich, Th., Buntic, I. (2003). *Very large eddy simulation for the prediction of unsteady vortex motion.* Conference on Modelling Fluid Flow (CMFF'03). 12th International Conference on Fluid Flow Technologies, Budapest, September 2003.
60. Hoffmann, H., Roswora, R. R., Egger, A. (2000). *Rectification of the Marsyangdi Trifurcation*. HydroVision 2000 (Charlotte, 2000).
61. Eichler, O. (1980). Vibration phenomena on hydraulic axial turbines. IAHR/IUTAM Symposium Karlsruhe, 1979, Paper B3. In E. Naudascher & D. Rockwell (Ed.), *Practical experiences with flow-induced vibrations*. Berlin: Springer.
62. Pulpitel, L. (1993). *The dynamic behaviour of a Kaplan turbine operating under non-standard conditions*. IAHR Work Group WG1 (The Behaviour of Hydraulic Machinery under Steady Oscillatory Conditions) 6th Meeting, Lausanne 1993.

http://www.springer.com/978-1-4471-4251-5

Flow-Induced Pulsation and Vibration in Hydroelectric Machinery
Engineer's Guidebook for Planning, Design and Troubleshooting

Dörfler, P.; Sick, M.; Coutu, A.

2013, XXIV, 244 p., Hardcover
ISBN: 978-1-4471-4251-5